ADVANCED MATERIALS TECHNOLOGIES

Supporting Information

for *Adv. Mater. Technol.*, DOI: 10.1002/admt.201900700

Modeling and Correcting Cure-Through in Continuous Stereolithographic 3D Printing

*Zachary D. Pritchard, Martin P.de Beer, Riley J. Whelan, Timothy F. Scott, and Mark A. Burns**

Supporting Information

Modelling and Correcting Cure-Through in Continuous Stereolithographic 3D Printing

*Zachary D. Pritchard, Martin P. de Beer, Riley J. Whelan, Timothy F. Scott, and Mark A. Burns**

S1. Materials and Methods

S1.1 Modeling and Correction

Computational models and slice correction algorithms were implemented in MATLAB R2018b (MathWorks) and run on a desktop computer (Intel Xeon E5-1660 v4 @ 3.2 GHz, 32 GB RAM). Simulations and corrections completed within several minutes for all models.

Dose Modeling: Slice images are initially read into the program and stored as a three-dimensional array. The dimensions of this array correspond to the number of slices and their dimensions in pixels. A typical slice image is 1,280 by 800 pixels and the number of slices is equal to the height of the designed part divided by the slicing height, h_s. In cases where the model does not utilize the full slice resolution (e.g., a 200-pixel-wide model in the center of a 1,280-pixel-wide image), the excess pixels outside the model volume are trimmed from the matrix to improve computational performance. The values in this matrix are grayscale pixel values (p) ranging from zero to one and correspond to the light intensities that will be projected at each pixel during each slice; zero and one represent the minimum and maximum blue-light intensities, respectively. The relationship between pixel value and light intensity is not linear, and pixel values are converted into intensities using a calibration curve (**Figure S1**) generated with a radiometer (International Light IL1400A).

Dose calculation begins at the bottom of the part, where the final slice is projected, and proceeds upward. The top cross-section of the part is exposed to every slice and each successive layer is exposed to fewer and fewer slices. By starting at the bottom of the part, we consider the cross-sections of the part exposed only to the final slice, then those exposed to the final two slices, then those exposed to the final three slices, and so on. As shown in Equation (5) and Table S2, the total dose at ζ is the sum of the dose contribution from slice $n = \zeta$ and the total dose at $\zeta + 1$ multiplied by a factor of $10^{-\eta}$.

Slice Correction: The unedited images from the slicing software are taken to represent the "true" model and are converted into matrix form as above. Each feature within the part is identified. As with dose modeling, slice correction begins at the bottom of the part and works upward. Pixel values at the backside of the feature are set to reach D_c as quickly as possible (i.e., using the maximum intensity), and pixel values inside the feature are set to match a desired internal dose profile using Equation (5). All pixel values are assumed to be zero (minimum intensity) unless specifically set otherwise. Finally, the matrix of corrected pixel values is converted back to a series of image files to be sent to the 3D printer.

S1.2 3D Printing

Part Design: Test parts were designed in DesignSpark Mechanical 2.0 (SpaceClaim Corp.) and exported as STL files. Models were sliced using Autodesk Netfabb Standard 2018 (Autodesk) with default settings for the Ember 3D Printer (Autodesk) and 10 μm slice height. Slices from Netfabb are used with the MATLAB code to model final printed parts and produce corrected slices.

3D Printer: We printed test parts on a previously-described dual-color continuous stereolithographic 3D printer.[1] The DLP LED projector (Optoma ML750) was modified by removing power to the green and red LEDs and powering the blue LED by an external 0-5A LED driver circuit controlled by a custom LabVIEW virtual instrument.

Resin Formulations: Polymer resin was formulated as a mixture of oligomer, reactive diluent, photoinitiators, photoinhibitor, and light absorbers. For this work, the oligomer Sartomer CN991 (Sartomer) was used with 1,6-hexanediol diacrylate (HDDA, TCI America) as a reactive diluent. (±)-Camphorquinone (CQ, Esstech) was used as a blue-light photoinitiator and ethyl-4-dimethylaminobenzoate (EDAB, Esstech) was used as a co-initiator. 2,2′-Bis(2-chlorophenyl)-4,4′,5,5′-tetraphenyl-1,2′-biimidazole (*o*-Cl-HABI, TCI America) was used as a UV-activated photoinhibitor. Epolight 5675 (Epolin) was used as the blue light absorber and

Tinuvin 328 (BASF) was used as the UV absorber. Commercial blue epoxy pigment (Makerjuice Labs) was also used as a light absorber. The compositions of resins used are given in **Table S1**.

Table S1. Resin formulations.

Component	Function	Concentration [wt%]		
		Resin 1	Resin 2	Resin 3
o-Cl HABI	photoinhibitor	2.8	2.8	2.8
camphorquinone	photoinitiator	1.9	1.9	1.9
EDAB	co-initiator	0.95	0.95	0.95
Tinuvin 328	UV absorber	0.47	0.47	0.47
Epolight 5675	blue light absorber	0.001	0.003	–
CN991	oligomer	56.3	56.3	56.3
HDDA	reactive diluent	37.6	37.6	37.6
blue pigment	light absorber	–	–	0.002

S1.3 Measurement of h_a and D_{gel}

The two resin properties required for input into the correction algorithm are the absorbance height h_a and the gelation dose D_{gel}. These properties are fitted using the least-squares method with a cured height vs. volumetric dose working curve similar to that developed by Jacobs[2]:

$$z_{ct} = h_a \log\left(\frac{I_0 t}{D_{gel}} \frac{\ln 10}{h_a} \right) \tag{S1}$$

Liquid photopolymer is cured into plugs by exposing to curing light of intensity I_0 for varying lengths of time t. The height of the cured plug is measured using a digital micrometer with an accuracy of 10 μm. Light intensities used in these experiments were measured using an International Light IL1400A radiometer with a GaAsP detector (model SEL005), a 10× attenuation neutral density filter (model QNDS1), and a quartz diffuser (model W).

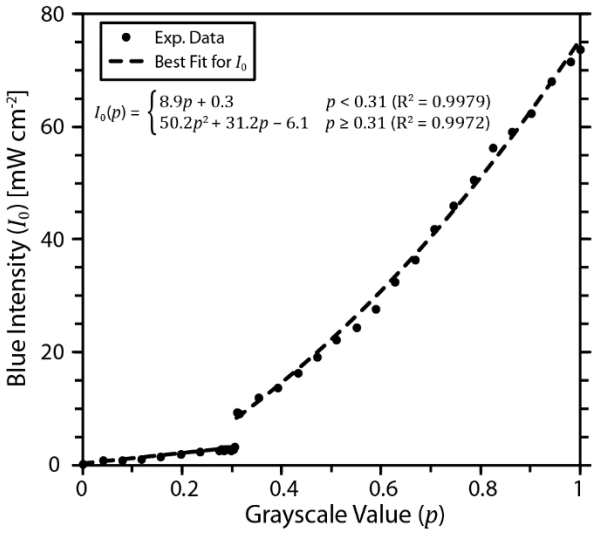

Figure S1. Measured blue intensity, I_0, as a function of the grayscale value, p, of the displayed image. The calibration curve is found to be a piece-wise function typical of manufacturer color balancing encoded into projector firmware.[3]

S2. Derivation of dose equations

S2.1 Derivation of main equations

The build platform begins in contact with the window and moves upward as the print proceeds. The coordinate system is defined with respect to the build platform, with $z = 0$ at the platform and increasing in the direction of the window (downward). Since the projected slices are patterned and intensity degrades as the light propagates, dose and intensity are functions of x, y, and z; however, for simplicity our notation will only include z with the understanding that each equation applies at a particular (x, y) position.

Printing consists of both continuous and discrete processes: as the build platform continuously ascends, exposure patterns change at discrete intervals with each slice projected in sequence. To account for the discrete projection of slices, the total accumulated dose at a point is a sum of contributions from each slice projected. $D_T(z)$ is the total dose delivered to position z in the final part; the contribution of slice n to the total dose is denoted as $D_n(z)$. Thus,

$$D_T(z) = \sum_{n=0}^{N} D_n(z) \tag{S2}$$

where slices are numbered from zero to N in the order of exposure.

To determine the dose contribution from each slice as the build platform continuously ascends, we will integrate over the time period when the slice is projected. The change in volumetric dose at a point is given by:

$$\frac{d}{dt} D_n(z,t) = -\frac{d}{dz} I_n(z,t) \tag{S3}$$

where t is time and I_n is the light intensity for slice n. The light intensity at any depth in the resin bath, $I_n(z)$, is given by Beer's Law. Recalling that $z = 0$ at the build platform, $z_w - z$ gives the distance from the position of the window (z_w) to the position of interest (z). From Beer's Law,

$$\frac{d}{dz} I_n(z,t) = -\frac{\ln 10}{h_a} I_{n,w} 10^{-[z_w(t)-z]h_a^{-1}} \tag{S4}$$

where $I_{n,w} = I_n(z_w)$ is the light intensity at the window and h_a is the resin absorbance height (the propagation distance over which the intensity falls to 10% of its initial value). Movement of the build platform is included via the print speed. Since the coordinate system is defined with respect to the build platform, the print speed s is represented in terms of the ever-increasing value of $z_w(t)$:

$$s = dz_w/dt \tag{S5}$$

Substituting Equation (S4) and (S5) into Equation (S3),

$$\frac{d}{dz_w} D_n(z, z_w) = \frac{\ln 10}{s h_a} I_{n,w} 10^{-[z_w(t)-z]h_a^{-1}} \tag{S6}$$

To calculate the dose contribution from slice n, Equation (S6) is integrated with respect to z_w. The limits of integration are the values of z_w when slice n is first projected and when the next slice, $n + 1$, is projected: nh_s and $(n + 1)h_s$, respectively, where h_s is the slicing height. Thus,

$$\begin{aligned} D_n(z) &= \int_{nh_s}^{(n+1)h_s} \frac{\ln 10}{s h_a} I_{n,w} 10^{-[z_w(t)-z]h_a^{-1}} dz_w \\ &= \frac{I_{n,w}}{s}\left\{10^{-(nh_s - z)h_a^{-1}} - 10^{-[(n+1)h_s - z]h_a^{-1}}\right\} \end{aligned} \tag{S7}$$

If the cross-section at height z is exposed to slice n (i.e., $z \leq nh_s$), Equation (S7) gives the contribution of slice n to the total dose at that point. If the cross-section is not exposed to slice n (i.e., $z \geq (n + 1)h_s$), the dose contribution is zero. As a simplification, we will consider only values of z which are multiples of h_s (i.e., z-values of simulated slices). For a treatment of all real values of z, see *Supporting Information S2.2* below. Note that this model implicitly assumes that a packet of resin tends to stay in the same (x, y, z)-position as the print progresses.

Combining Equation (S2) and (S7),

$$D_T(z) = \sum_{n=zh_s^{-1}}^{N} \frac{I_{n,w}}{s}\left\{10^{-(nh_s - z)h_a^{-1}} - 10^{-[(n+1)h_s - z]h_a^{-1}}\right\} \tag{S8}$$

Equation (S8) allows calculation of the total accumulated dose at any point in the final printed part.

For convenience we may define several dimensionless variables. The dimensionless dose, Ω, is normalized by the critical dose, D_c:

$$\Omega_n \equiv \frac{D_n}{D_c} \tag{S9}$$

The critical dose is experimentally determined for each resin formulation and is related to the dose at which the resin becomes insoluble in the rinse solvent, IPA (i.e., reaches the gelation point). A resin packet with $\Omega_T < 1$ is considered uncured, while resin with $\Omega_T \geq 1$ is considered cured. The dimensionless light intensity at the window, Φ, is normalized by a critical intensity; I_c is the minimum intensity at which it is possible to reach D_c for h_a and s (for additional discussion, see *Supporting Information S2.3* below).

$$\Phi_n \equiv \frac{I_{n,w}}{I_c} = \frac{I_{n,w}}{D_c s} \tag{S10}$$

The dimensionless *z*-position, ζ, is normalized by the slice height:

$$\zeta \equiv \frac{z}{h_s} \tag{S11}$$

With this normalization, slice *n* is first projected when $\zeta_w = n$. Finally, the dimensionless constant η is the ratio of the slicing height to the absorbance height:

$$\eta \equiv \frac{h_s}{h_a} \tag{S12}$$

Rewriting Equation (S8) in dimensionless terms,

$$\Omega_T(\zeta) = \sum_{n=\zeta}^{N} \Phi_n \left\{ 10^{-(n-\zeta)\eta} - 10^{-\left[(n+1)-\zeta\right]\eta} \right\} \tag{S13}$$

As derived in *Supporting Information S2.4* below, Equation (S13) can be simplified such that $\Omega_T(\zeta)$ is a function of $\Omega_T(\zeta + 1)$:

$$\Omega_T(\zeta) = \Phi_\zeta \left(1 - 10^{-\eta}\right) + \Omega_T(\zeta + 1) 10^{-\eta} \tag{S14}$$

In Equation (S14), we find the relationship that will allow quick dose calculation and slice correction. Starting at the end of the part (i.e., $\zeta = N$), we may calculate the total dose in each

layer sequentially by considering only the current layer and the preceding layer. Table S2 gives expressions for Ω_T at several values of ζ.

Table S2. Total dose by layer from Equation (S14).

ζ	$\Omega_T(\zeta)$
N	$\Phi_N\left(1-10^{-\eta}\right)$
$N-1$	$\Phi_{N-1}\left(1-10^{-\eta}\right)+\Omega_T(N)10^{-\eta}$
…	…
0	$\Phi_0\left(1-10^{-\eta}\right)+\Omega_T(1)10^{-\eta}$

S2.2 Fractional values of ζ

When non-integer values of ζ are considered, there are three important cases for determining the value of $\Omega_n(\zeta)$. Recalling that ζ_w, the window position, increases constantly as the build platform ascends, these cases are delineated by the value of ζ and the values of ζ_w while the slice n is projected. As noted above, $\zeta_w = n$ when slice n is first projected, and the next slice is projected at $\zeta_w = n + 1$.

With the ζ_w values for each slice known, we may consider the three cases for $\Omega_n(\zeta)$. In the first case, the cross-section at ζ is never exposed while slice n is projected (i.e., $\zeta_w < \zeta$ during the entire period slice n is projected). Here, the value of $\Omega_n(\zeta)$ is simply zero.

$$\Omega_n(\zeta) = 0, \quad n+1 < \zeta \le N \tag{S15}$$

with N corresponding to the final slice.

In the second case, the cross-section at ζ is first exposed during slice n (i.e., $\zeta_w = \zeta$ at some point while the slice is projected). To handle this case will require a more generic form of Equation (S7). Considering a constant exposure from $z_w = z_{w,1}$ to $z_w = z_{w,2}$:

$$\frac{d}{dz_w} D(z, z_w) = \frac{\ln 10}{s h_a} I_{n,w} 10^{-\left[z_w(t)-z\right]h_a^{-1}} \tag{S16}$$

$$D(z) = \int_{z_{w,1}}^{z_{w,2}} \frac{\ln 10}{s h_a} I_{n,w} 10^{-[z_w(t)-z]h_a^{-1}} dz_w$$

$$= \frac{I_{n,w}}{s}\left[10^{-(z_{w,1}-z)h_a^{-1}} - 10^{-(z_{w,2}-z)h_a^{-1}} \right] \quad \text{(S17)}$$

$$\Omega(\zeta) = \Phi\left[10^{-(\zeta_{w,1}-\zeta)\eta} - 10^{-(\zeta_{w,2}-\zeta)\eta} \right] \quad \text{(S18)}$$

For this case, the dose contribution is zero while $\zeta_w < \zeta$. Integrating Equation (S18) with limits $\zeta_{w,1} = \zeta$ and $\zeta_{w,2} = n + 1$,

$$\Omega_n(\zeta) = \Phi_n\left\{ 10^{-(\zeta-\zeta)\eta} - 10^{-\lceil (n+1)-\zeta \rceil \eta} \right\}, \quad n < \zeta \le n+1$$

$$= \Phi_n\left\{ 1 - 10^{-\lceil (n+1)-\zeta \rceil \eta} \right\} \quad \text{(S19)}$$

In the final case, ζ is exposed for the entire duration of the slice (i.e., $\zeta_w > \zeta$ during the entire period slice n is projected). Here, Equation (S18) applies with $\zeta_{w,1} = n$ and $\zeta_{w,2} = n + 1$.

$$\Omega_n(\zeta) = \Phi_n\left\{ 10^{-(n-\zeta)\eta} - 10^{-\lceil (n+1)-\zeta \rceil \eta} \right\}, \quad 0 \le \zeta \le n \quad \text{(S20)}$$

Combining Equation (S15), (S19), and (S20) into a single expression for $\Omega_n(\zeta)$,

$$\Omega_n(\zeta) = \begin{cases} 0, & n+1 < \zeta \le N \\ \Phi_n\left\{ 1 - 10^{-\lceil (n+1)-\zeta \rceil \eta} \right\}, & n < \zeta \le n+1 \\ \Phi_n\left\{ 10^{-(n-\zeta)\eta} - 10^{-\lceil (n+1)-\zeta \rceil \eta} \right\}, & 0 \le \zeta \le n \end{cases} \quad \text{(S21)}$$

Equation (S21) allows us to determine the contribution of any particular slice to the dose at any point.

To use Equation (S2) with a non-integer value of ζ, it is necessary to rewrite the conditions in Equation (S21). Using floor bracket notation, where $\lfloor \zeta \rfloor$ indicates the value of ζ rounded *down* to the nearest integer, the first case occurs for $0 \le n < \lfloor \zeta \rfloor$, the second case occurs only for $n = \lfloor \zeta \rfloor$, and the third case occurs for $\lfloor \zeta \rfloor < n \le N$. Rewriting Equation (S21) with these conditions:

$$\Omega_n(\zeta) = \begin{cases} 0, & 0 \le n < \lfloor \zeta \rfloor \\ \Phi_n \left\{ 1 - 10^{-\lceil (n+1)-\zeta \rceil \eta} \right\}, & n = \lfloor \zeta \rfloor \\ \Phi_n \left\{ 10^{-(n-\zeta)\eta} - 10^{-\lceil (n+1)-\zeta \rceil \eta} \right\}, & \lfloor \zeta \rfloor < n \le N \end{cases} \quad \text{(S22)}$$

Applying Equation (S22) to Equation (S2),

$$\Omega_T(\zeta) = \Phi_{\lfloor \zeta \rfloor} \left[1 - 10^{-(\lfloor \zeta \rfloor - \zeta)\eta} \right] + \sum_{n=\lfloor \zeta \rfloor + 1}^{N} \Phi_n \left\{ 10^{-(n-\zeta)\eta} - 10^{-\lceil (n+1)-\zeta \rceil \eta} \right\} \quad \text{(S23)}$$

Equation (S23) allows calculation of the total dose at non-integer values of ζ.

S2.3 Critical intensity I_c and dimensionless intensity Φ

I_c is defined as the minimum intensity for which it is possible to reach the critical dose. This theoretical limit is reached for an infinitely long exposure—that is, when exposure occurs over a z_w range from z to infinity. Integrating Equation (S16) with these limits,

$$\begin{aligned} D_c &= \int_z^{\infty} \frac{\ln 10}{s h_a} I_{n,w} 10^{-(z_w - z) h_a^{-1}} dz_w \\ &= \frac{I_c}{s} \left[10^{-(z-z) h_a^{-1}} - 10^{-(\infty - z) h_a^{-1}} \right] \\ &= \frac{I_c}{s} (1 - 0) \\ &= \frac{I_c}{s} \end{aligned} \quad \text{(S24)}$$

Rearranging and substituting into Φ,

$$I_c = D_c s \quad \text{(S25)}$$

$$\Phi_n \equiv \frac{I_{n,w}}{I_c} = \frac{I_{n,w}}{D_c s} \quad \text{(S26)}$$

Similarly, Φ defines the asymptotic value of the dose as the exposure time tends to infinity. Substituting $\zeta_{w,1} = \zeta$ and $\zeta_{w,1} = \infty$ into Equation (S18),

$$\begin{aligned} \Omega_{\infty}(\zeta) &= \Phi \left[10^{-(\zeta - \zeta)\eta} - 10^{-(\infty - \zeta)\eta} \right] \\ &= \Phi (1 - 0) \\ &= \Phi \end{aligned} \quad \text{(S27)}$$

S2.4 Dependence of $\Omega_T(\zeta)$ on $\Omega_T(\zeta+1)$

If we contrast the total doses at ζ and ζ + 1, we will find that the doses are interrelated. $\Omega_T(\zeta)$ is given by Equation (S2):

$$\begin{aligned}\Omega_T(\zeta) &= \sum_{n=\zeta}^{N} \Omega_n(\zeta) \\ &= \Omega_\zeta(\zeta) + \sum_{n=\zeta+1}^{N} \Omega_n(\zeta)\end{aligned} \tag{S28}$$

Here, the sum has been split into two terms: first, the contribution from slice ζ and second, the contributions from all remaining slices. Looking more closely at the second term:

$$\begin{aligned}\Omega_n(\zeta) &= \Phi_n \left\{ 10^{-(n-\zeta)\eta} - 10^{-\left[(n+1)-\zeta\right]\eta} \right\}, \quad \zeta + 1 \le n < N \\ &= \Phi_n \left\{ 10^{-\left[n-(\zeta+1)\right]\eta} - 10^{-\left[(n+1)-(\zeta+1)\right]\eta} \right\} 10^{-\eta} \\ &= \Omega_n(\zeta+1)10^{-\eta}\end{aligned} \tag{S29}$$

Equation (S29) shows that the contribution of slice *n* (where $n \ge \zeta$) to the dose at ζ is equivalent to the contribution of slice *n* to the dose at ζ + 1, multiplied by a factor of $10^{-\eta}$. Substituting back into Equation (S28),

$$\Omega_T(\zeta) = \Omega_\zeta(\zeta) + \sum_{n=\zeta+1}^{N} \Omega_n(\zeta+1)10^{-\eta} \tag{S30}$$

Considering the left term:

$$\begin{aligned}\Omega_\zeta(\zeta) &= \Phi_\zeta \left\{ 10^{-(\zeta-\zeta)\eta} - 10^{-\left[(\zeta+1)-\zeta\right]\eta} \right\} \\ &= \Phi_\zeta \left(1 - 10^{-\eta} \right)\end{aligned} \tag{S31}$$

And the right:

$$\begin{aligned}\sum_{n=\zeta+1}^{N} \Omega_n(\zeta+1)10^{-\eta} &= 10^{-\eta} \sum_{n=\zeta+1}^{N} \Omega_n(\zeta+1) \\ &= 10^{-\eta}\, \Omega_T(\zeta+1)\end{aligned} \tag{S32}$$

On recombination,

$$\Omega_T(\zeta) = \Phi_\zeta \left(1 - 10^{-\eta}\right) + \Omega_T(\zeta + 1)10^{-\eta} \tag{S33}$$

In Equation (S33), we find the relationship that will allow quick dose calculation and slice correction. Starting at the end of the part (i.e., $\zeta = N$) and moving upward slice-by-slice, we may calculate the cumulative dose in each layer sequentially by considering only the current layer and the preceding layer. Table S2 gives expressions for Ω_T at several values of ζ.

S3. Effect of finite contrast ratio

A deeper examination of behavior while black pixels are projected will highlight the significance of the projector contrast ratio. The contrast ratio of a display system is defined as the ratio of intensities for white and black; this is a finite quantity since pure black (i.e., an irradiance of zero) is unachievable. Consider a point ζ in the part envelope with a corresponding grayscale pixel value—that is, the pixel value for slice $n = \zeta$—is zero. From Equation (S14), the total dose at this position depends on the minimum intensity and the total dose of the layer below:

$$\Omega_T(\zeta) = \Phi_{min}\left(1 - 10^{-\eta}\right) + \Omega_T(\zeta + 1)10^{-\eta} \tag{S34}$$

When the dose contribution from the minimum intensity matches the exponential decay from the dose at $\zeta + 1$, a constant dose is maintained:

$$\begin{aligned} \Omega_{min} &= \Phi_{min}\left(1 - 10^{-\eta}\right) + \Omega_{min}10^{-\eta} \\ &= \Phi_{min} \end{aligned} \tag{S35}$$

This dose, Ω_{min}, acts as an effective minimum dose: if $\Omega_T \geq \Omega_{min}$ at position (x_0, y_0, z_0), then $\Omega_T \geq \Omega_{min}$ for all points (x_0, y_0, $z \leq z_0$). The minimum dose is determined by the resin properties and the print speed as well as the contrast ratio of the projection system. For our printer, we have measured a minimum intensity of 1 mW cm^{-2}, resulting in a minimum dose of approximately 36 mJ cm^{-3} (varying with other parameters).

S4. Equations for target dose region constraints

In a region of constant-intensity exposure, the dose at any point can be calculated if the dose at one point is known. If ζ_0 and Ω_0 are the known position and dose and Φ_0 is the constant intensity,

$$\Omega(\zeta) = \Omega_0 10^{-(\zeta_0-\zeta)\eta} + \Phi_0\left[1-10^{-(\zeta_0-\zeta)\eta}\right] \tag{S36}$$

For the constraint curves defining target dose regions, each curve has a constant intensity exposure (Φ_{max} for constraint *(ii)* and Φ_{min} for constraint *(iii)*), and the dose at the top and bottom edges are known (Ω_c). If the upper and lower edges of the feature are located at ζ_U and ζ_L (see **Figure S2**),

$$\Omega_{ii}(\zeta) = \Omega_c 10^{-(\zeta_L-\zeta)\eta} + \Phi_{max}\left[1-10^{-(\zeta_L-\zeta)\eta}\right] \tag{S37}$$

$$\Omega_{iii}(\zeta) = \Omega_c 10^{-(\zeta_U-\zeta)\eta} + \Phi_{min}\left[1-10^{-(\zeta_U-\zeta)\eta}\right] \tag{S38}$$

The constraint curves, and thus the target dose region, are dependent on several system parameters. The relative effect of a change in each parameter is shown below in **Figure S3**.

In Figure 3, we compare dose profiles with varying maximum doses; however, the chosen maximum dose may not be reached for some features. As is evident from Figure S3, several factors determine the shape of the target dose region for a feature. While most parameters are constant throughout the print (I_{max}, s, and h_a), the feature size may vary considerably. For a constant set of system parameters, each feature has a maximum achievable Ω_{max} as a function of its height. To determine this value, Equations (S37) and (S38) are first equated to determine the point at which the curves meet.

$$\zeta^* = \frac{1}{\eta}\log_{10}\left[\frac{\Phi_{max}-\Phi_{min}}{\left(\Omega_c-\Phi_{min}\right)10^{-\zeta_U\eta}-\left(\Omega_c-\Phi_{max}\right)10^{-\zeta_L\eta}}\right] \tag{S39}$$

Using Equation (S39), we can write the maximum dose (assuming the edges are at the critical dose) as a function of feature height.

$$\delta \equiv \zeta_L - \zeta_U \tag{S40}$$

$$\begin{aligned}\zeta^* &= \frac{1}{\eta}\log_{10}\left[\frac{\Phi_{max}-\Phi_{min}}{(\Omega_c-\Phi_{min})10^{-\zeta_U\eta}-(\Omega_c-\Phi_{max})10^{-(\zeta_U+\delta)\eta}}\right] \\ &= \frac{1}{\eta}\log_{10}\left[\frac{\Phi_{max}-\Phi_{min}}{(\Omega_c-\Phi_{min})-(\Omega_c-\Phi_{max})10^{-\delta\eta}}\frac{1}{10^{-\zeta_U\eta}}\right] \\ &= \frac{1}{\eta}\log_{10}\left[\frac{\Phi_{max}-\Phi_{min}}{(\Omega_c-\Phi_{min})-(\Omega_c-\Phi_{max})10^{-\delta\eta}}\right]-\frac{1}{\eta}\log_{10}\left(10^{-\zeta_U\eta}\right) \\ &= \frac{1}{\eta}\log_{10}\left[\frac{\Phi_{max}-\Phi_{min}}{(\Omega_c-\Phi_{min})-(\Omega_c-\Phi_{max})10^{-\delta\eta}}\right]+\zeta_U \end{aligned} \quad \text{(S41)}$$

Substituting Equation (S41) into Equation (S38),

$$\Omega^* \equiv \Omega(\zeta^*) = \frac{(\Omega_c-\Phi_{min})(\Phi_{max}-\Phi_{min})}{(\Omega_c-\Phi_{min})-(\Omega_c-\Phi_{max})10^{-\delta\eta}}+\Phi_{min} \quad \text{(S42)}$$

Figure S4 shows Ω* as a function of feature height.

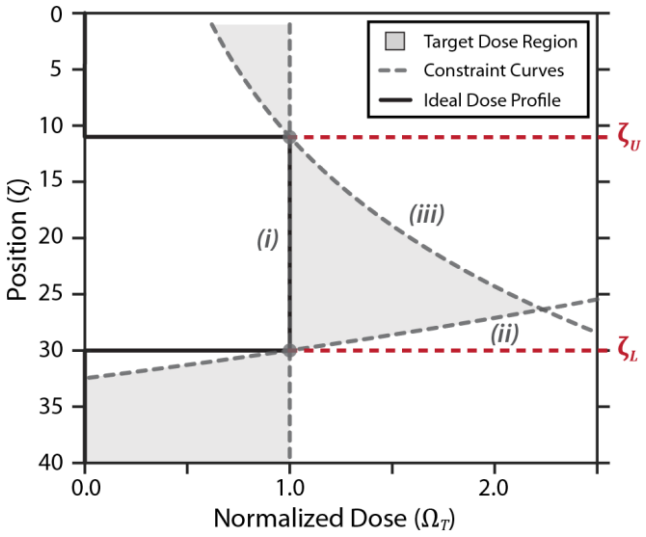

Figure S2. Dose constraint curves *(i)–(iii)* and target dose region. ζ_U and ζ_L are the positions of the top and bottom of the feature, respectively.

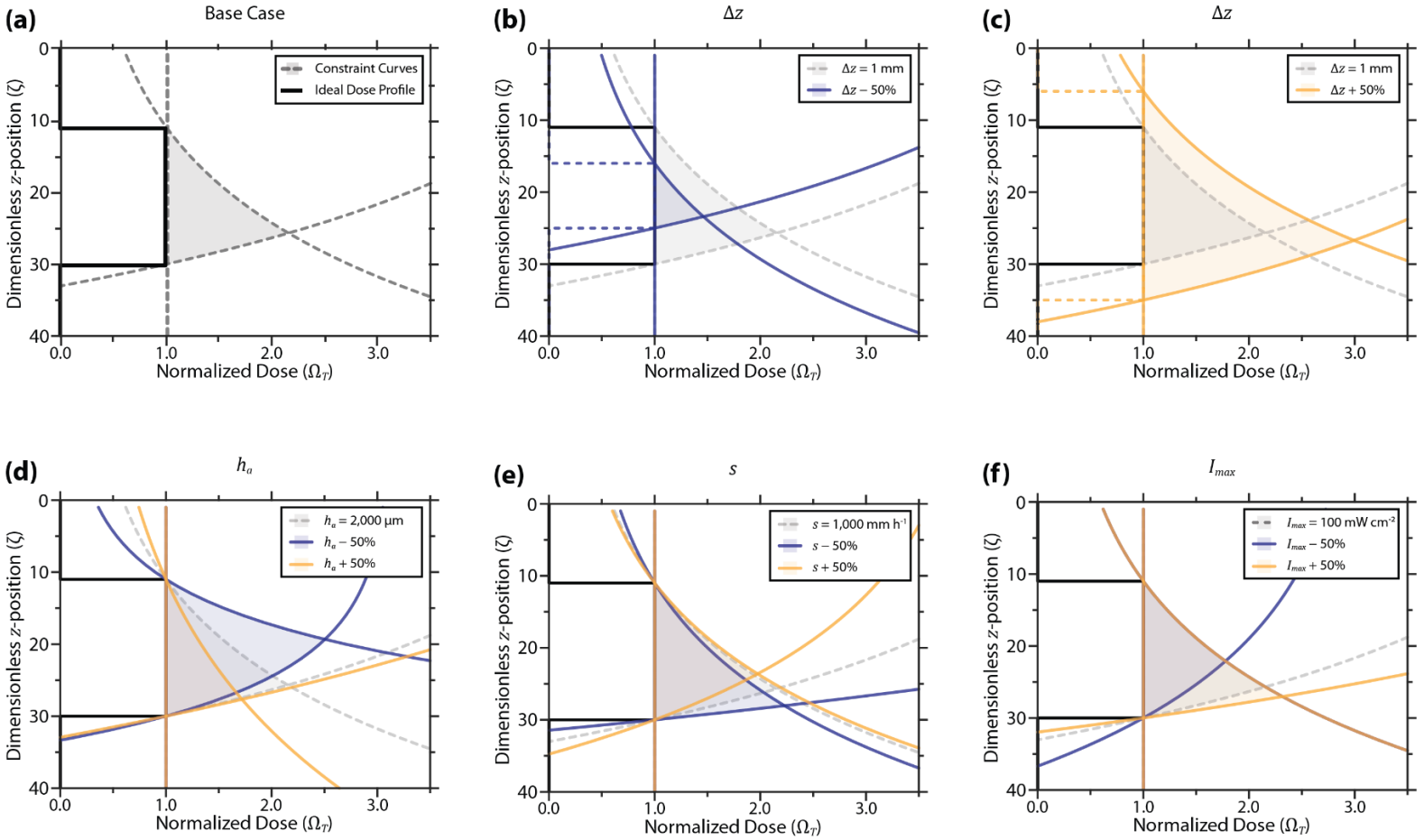

Figure S3. Effect of increasing (yellow curves) and decreasing (blue curves) parameters by 50%: **(a)** Base case. h_s = 50 µm, Δz = 1 mm, h_a = 2,000 µm, s = 1,000 mm h^{-1}, and I_{max} = 100 mW cm^{-2}. **(b)** Decreasing feature height. **(c)** Increasing feature height. **(d)** Varying absorbance height. **(e)** Varying print speed. From Equation (S10), varying the critical dose has an identical effect. **(f)** Varying the maximum projector intensity.

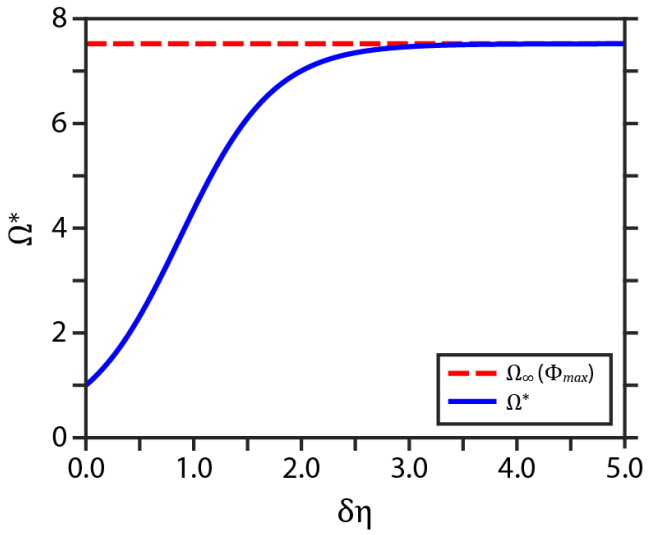

Figure S4. Maximum dose as a function of $\delta\eta = (z_L - z_U)h_a^{-1}$. As the feature height increases, the maximum dose approaches the limit Ω_∞ described in *Supporting Information S2.3*. Parameters: h_s = 50 μm, h_a = 2,000 μm, s = 1,000 mm h^{-1}, I_{max} = 120 mW cm^{-2}, I_{min} = 2 mW cm^{-2}.

S5. Optimizing D_c and Ω_{max}

Effective slice correction requires that correction parameters are optimized for the resin being used. **Figure S5** illustrates two limits on the maximum achievable dose for printing with Resin 1 at 750 mm h^{-1}; these limits exist independently from the chosen value of Ω_{max}. As discussed in *Supporting Information S2.3*, an infinitely long exposure at Φ asymptotically approaches the dose $\Omega_\infty(\Phi)$. Thus, the maximum intensity defines a maximum possible dose in the model: $\Omega_\infty(\Phi_{max}) = \Phi_{max}$. Figure S5(a) shows the distance that must be exposed at the maximum intensity before the critical dose is reached. This relationship suggests than certain feature-dense geometries may not be amenable to correction with these print settings; however, slower print speeds or higher light intensities may be used to compress the curve downward (for a constant exposure height, $D \propto Is^{-1}$).

For individual features, the maximum dose is the lesser of the prescribed Ω_{max} and Ω^* as defined in Supporting Information S4. Analogous to Figure S4, Figure S5(b) shows D^*/ D_{gel} as a function of feature height for Resin 1 at 750 mm h^{-1} and several values of D_c.

In addition to optimizing the critical dose parameter D_c, we also conducted experiments investigating the effect of the maximum dose parameter Ω_{max}, with results shown in **Figure S6**. Setting higher values of D_{max} makes the fidelity less sensitive to feature size, though the effect is minor. Based on this result and the desire to maximize green strength, we chose to operate the correction with an unconstrained maximum dose ($\Omega_{max} = \infty$).

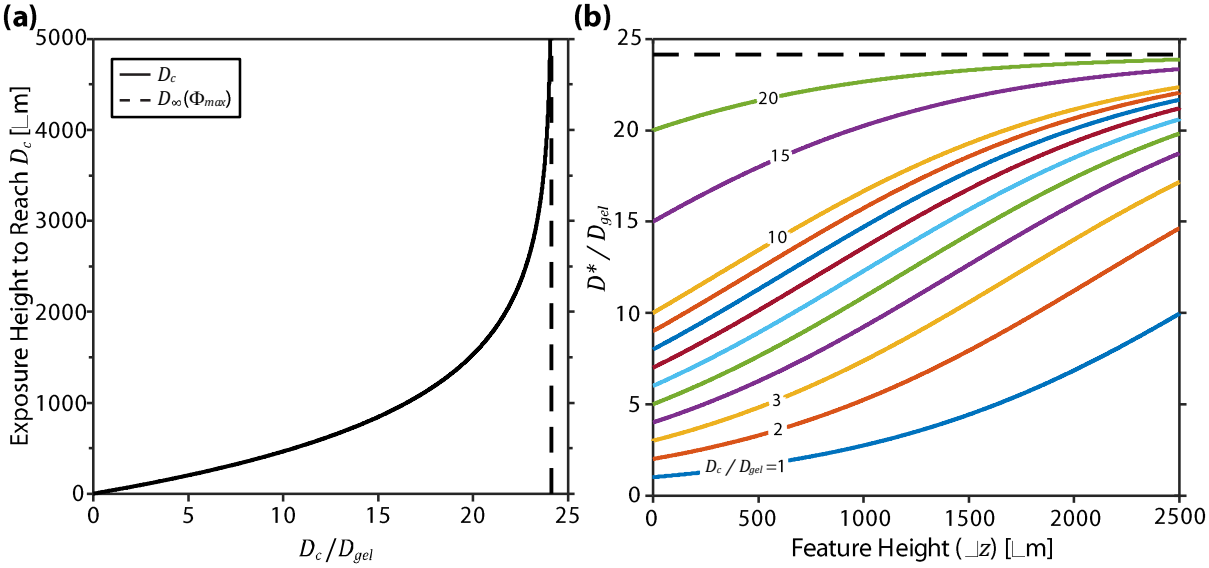

Figure S5. Maximum dose limits for our presented optimization (Resin 1, s = 750 mm h^{-1}, I_{max} ≈ 75 mW cm^{-2}). **(a)** Exposure height to reach the critical dose starting from zero dose. Printing at a constant speed, larger height ranges must be exposed to reach higher doses. **(b)** The maximum possible dose for a feature of a given height, as determined by the dose constraint equations (Equation (S42) in Supporting Information S4). When the correction is applied, the maximum dose within a feature is the minimum of D^* and the chosen D_{max}.

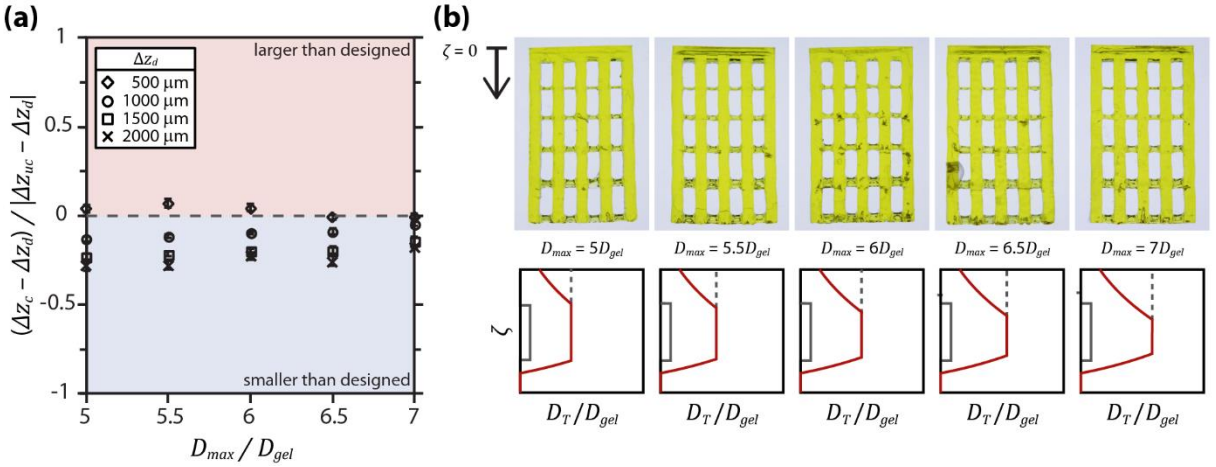

Figure S6. Varying D_{max} with D_c = 5D_{gel}. **(a)** Ratio of height errors (corrected-to-uncorrected) for a range of feature sizes and values of D_{max}. A ratio of zero corresponds to a perfectly corrected feature. Error bars indicate standard error. **(b)** Parts printed at 750 mm h^{-1} using slices corrected with D_c = 5D_{gel} and different values for D_{max}.

S6. Model and correction for non-continuous stereolithography

While the main body of this work relates to continuous stereolithography, we present here an adapted model and correction approach for use with traditional layer-by-layer stereolithography. Our dose model is similar to those previously reported.[4,5] While grayscale has previously been used to improve x-y resolution,[6] it has not, to our knowledge, been explored as a solution for cure-through. The *compensation zone* approach was partly developed to address cure-through artifacts on exterior features by adjusting the dimensions of the model through an optimization process.[7,8] A compensation-zone-like approach was subsequently developed for internal voids.[9] Manual adjustments to account for cure-through have also been reported.[10] These references also provide background on the layer-by-layer printing process for unfamiliar readers.

S6.1 Derivation of dose model

As in the continuous case, the total dose at a point is the sum of contributions from all slices.

$$D_T(z) = \sum_{n=0}^{N} D_n(z) \tag{S43}$$

$$\begin{aligned} \frac{d}{dt} D_n(z,t) &= -\frac{d}{dz} I_n(z,t) \\ &= \frac{\ln 10}{h_a} I_{n,w} 10^{-(nh_s - z)h_a^{-1}} \end{aligned} \tag{S44}$$

For layer-by-layer exposure, each slice is exposed for time t_e while the build platform is stationary. For slices to which position z is not exposed ($n < zh_s^{-1}$), $D_n(z) = 0$. If z is exposed to slice n ($n \geq zh_s^{-1}$), the dose is given by:

$$\begin{aligned} D_n(z) &= \int_0^{t_e} \frac{\ln 10}{h_a} I_{n,w} 10^{-(nh_s - z)h_a^{-1}} dt \\ &= \frac{\ln 10}{h_a} I_{n,w} 10^{-(nh_s - z)h_a^{-1}} t_e \end{aligned} \tag{S45}$$

$$D_T(z) = \sum_{n=\lceil zh_s^{-1} \rceil}^{N} \frac{\ln 10}{h_a} I_{n,w} 10^{-(nh_s - z)h_a^{-1}} t_e \tag{S46}$$

Dimensionless variables for the layer-by-layer model are identical to those used in the continuous model with the exception of dimensionless intensity, which is now

$$\Phi'_n \equiv \frac{I_{n,w}}{I'_c} = \frac{I_{n,w} t_e \ln 10}{D_c h_a} \tag{S47}$$

Substituting dimensionless variables into Equation (S46),

$$\Omega_T(\zeta) = \sum_{n=\lceil \zeta \rceil}^{N} \Phi'_n 10^{-(n-\zeta)\eta} \tag{S48}$$

Equation (S48) can be used to calculate the total accumulated dose at any point in a part printed using layer-by-layer stereolithography.

S6.2 Slice correction

In non-continuous stereolithography, the exposure time is set such that the far edge of the current layer reaches the critical dose. In our notation, this position is $\zeta = n - 1$ for each slice n. Since the points of interest are integer values of ζ, we may perform a simplification analogous to Equation (S33) from the continuous case to assist in correction:

$$\Omega_c = \Phi'_{\zeta+1} 10^{-\eta} + \Omega_T(\zeta + 2) 10^{-2\eta} \tag{S49}$$

As with the continuous case, the correction is performed starting at the end of the part ($\zeta = N$) and moving upward slice-by-slice. From Equation (S49), the intensity required to reach the critical dose can be determined for each layer within a designed feature.

We applied the dose model and slice correction for layer-by-layer stereolithography to a test model identical to that used in Figure 2 and 4. Figure S7(a – d) shows the model results for uncorrected slices, while Figure S7(e – h) shows the results for corrected slices. These results, along with the discussion below, show how slice correction can be used in combination with resin and printer optimization to minimize cure-through in non-continuous stereolithography.

For both corrected and uncorrected slices, a characteristic sawtooth pattern resulting from discontinuous build platform motion is evident in the dose profile. These discontinuities together with the nonzero background intensity of the projection system have the effect of preventing "perfect" correction using our method. If the top edge of a feature is just at the critical dose, there will be cure-through into the region just above it resulting from additional exposure at the minimum intensity. The height of the minimum cure-through region, z_{CT} (dimensionless: ζ_{CT}), is a function of resin and system parameters and can be calculated. The dose at the top and bottom boundaries of the cure-through region is equal to Ω_c, and the projector is at the minimum intensity:

$$\Omega_c = \Phi'_{min} 10^{-\zeta_{CT}\eta} + \Omega_c 10^{-\zeta_{CT}\eta} \tag{S50}$$

$$\zeta_{CT} = \frac{1}{\eta} \log\left(\frac{\Phi'_{min}}{\Omega_c} + 1 \right) \tag{S51}$$

$$z_{CT} = h_a \log\left(\frac{I_{min} t_e \ln 10}{D_c h_a} + 1 \right) \tag{S52}$$

If the exposure time is chosen such that the back edge of a feature just reaches the critical dose when exposed at maximum intensity,

$$t_e = \frac{D_c}{I_{max} 10^{-h_s h_a^{-1}}} \frac{h_a}{\ln 10} \tag{S53}$$

$$z_{CT} = h_a \log\left(\frac{I_{min}}{I_{max}} 10^{h_s h_a^{-1}} + 1 \right) \tag{S54}$$

Thus, the size of the minimum cure-through region in layer-by-layer stereolithography is a function of the resin absorbance height, the layer height, and the projector contrast ratio. The amount of cure-through for a corrected model is reduced by using a high-contrast-ratio projection system and a small layer thickness. Once these parameters are set, the resin absorbance height can be optimized to minimize z_{CT} using Equation (S54). For the parameters used in Figure S7, $z_{CT} \approx 5$ μm.

Figure S7 also highlights the dose heterogeneity inherent to non-continuous stereolithography. We can define the degree of dose heterogeneity ω as the ratio of maximum to minimum dose within a layer:

$$\begin{aligned}\omega &= \frac{\Omega_T(\zeta)}{\Omega_T(\zeta)10^{-\eta}} \\ &= 10^{h_s h_a^{-1}}\end{aligned} \tag{S55}$$

The degree of dose heterogeneity thus increases as the layer height increases and decreases as the absorbance height increases. For the hypothetical resin in Figure S7, ω = 2.848.

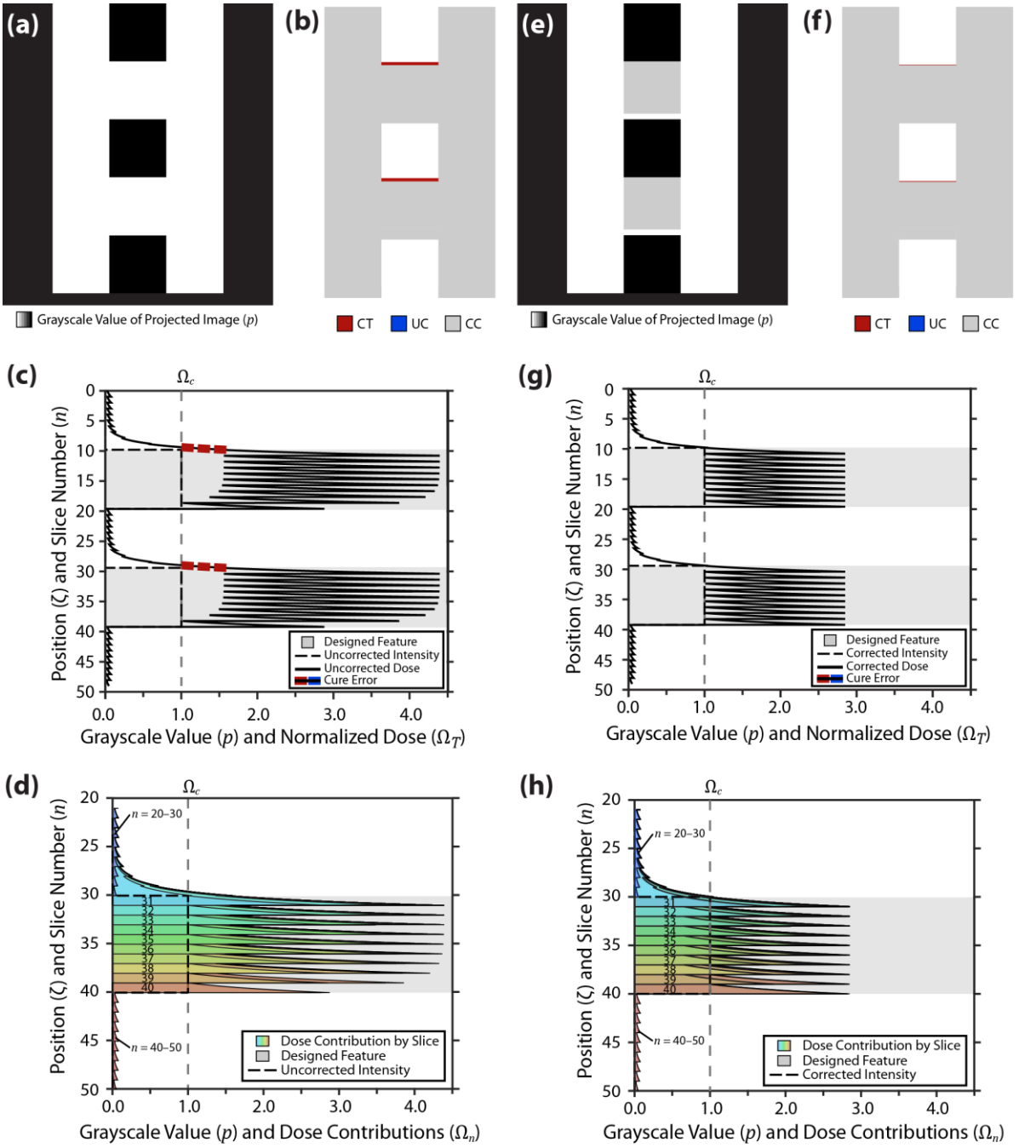

Figure S7. Layer-by-layer printing of 3D model in Figure 2(a). D_c = 576 mJ cm^{-3}, h_s = 50 µm, h_a = 110 µm, and s = 1,000 mm h^{-1}. **(a)** Vertical stack of uncorrected grayscale projections along the plane indicated in Figure 2(a). **(b)** Model prediction from slices in (a) showing areas with cure-through (CT, red). Gray regions of the part are correctly cured (CC). **(c)** Grayscale value and dose for the (x, y) position indicated by the dashed line in Figure 2(a). **(d)** Contributions of individual slices to the accumulated dose curve shown in (c) for n = 21 to n = 53. **(e–h)** Results for corrected slices.

References

[1] M. P. de Beer, H. L. van der Laan, M. A. Cole, R. J. Whelan, M. A. Burns, T. F. Scott, *Sci. Adv.* **2019**, *5*, eaau8723.

[2] P. F. Jacobs, *Rapid Prototyping & Manufacturing: Fundamentals of Stereolithography*, Society Of Manufacturing Engineers, Dearborn, Michigan, **1992**.

[3] M. C. Stone, in *9th Color Imaging Conf. Final Progr. Proc.*, **2001**, pp. 342–347.

[4] H. Gong, M. Beauchamp, S. Perry, A. T. Woolley, G. P. Nordin, *RSC Adv.* **2015**, *5*, 3627.

[5] H. Gong, B. P. Bickham, A. T. Woolley, G. P. Nordin, *Lab Chip* **2017**, *17*, 2899.

[6] C. Zhou, Y. Chen, R. A. Waltz, *J. Manuf. Sci. Eng.* **2009**, *131*, 1.

[7] A. S. Limaye, D. W. Rosen, *Rapid Prototyp. J.* **2006**, *12*, 283.

[8] A. S. Limaye, D. W. Rosen, *Rapid Prototyp. J.* **2007**, *13*, 76.

[9] P. F. O'Neill, N. Kent, D. Brabazon, *AIP Conf. Proc.* **2017**, *200012*, DOI 10.1063/1.5008249.

[10] M. J. Männel, L. Selzer, R. Bernhardt, J. Thiele, *Adv. Mater. Technol.* **2019**, *4*, 1800408.